

## Action of Polymyxin B on Bacterial Membranes: Morphological Changes in the Cytoplasm and in the Outer Membrane of *Salmonella typhimurium* and *Escherichia coli* B

PETER R. G. SCHINDLER AND MICHAEL TEUBER\*

Department of Microbiology, Technical University of Munich, D-8000 Munich 2, Germany

Received for publication 24 March 1975

Though the primary action of the cationic antibiotic polymyxin B is against the membrane of susceptible bacteria, severe morphological changes are detected in the cytoplasm. Using fluorescence microscopy and a mono-*N*-dansyl-polymyxin B derivative, we could demonstrate aggregations of the antibiotic with cellular material, possibly nucleic acids and/or ribosomes. These aggregations were only produced by minimum inhibitory or higher concentrations of the antibiotic as shown with *Salmonella* and *Escherichia* strains differing in their polymyxin susceptibility. The outer membrane of *Salmonella typhimurium* revealed characteristic blebs when treated with polymyxin B. This was investigated by the gentle methods of spray-freezing and freeze-etching. The obtained electron micrographs suggest that the polymyxin-induced blebs are projections of the outer monolayer of the outer membrane. A possible mechanism of penetration of polymyxin B through the cell envelope of gram-negative bacteria is presented.

The basic polypeptide polymyxin B (PX) acts specifically on gram-negative bacteria by electrostatic and hydrophobic interactions with anionic cell envelope components like phospholipids (10, 11, 21, 34, 36) and lipopolysaccharides (LPS) (3, 26). These molecules are most likely the primary receptor molecules and responsible for the classification of the polymyxins as membrane-specific antibiotics. A possible penetration of the antibiotic into the cytoplasm, however, has not been directly demonstrated, although Few and Schulmann (7) supposed from binding studies that such a penetration could occur. In the same sense, Handley et al. (9) interpreted the condensation of nuclear material in PX-treated bacteria as revealed by electron microscopy as polymyxin-deoxyribonucleic acid complexes. These have been described in vitro (18). By the use of mono-*N*-dimethylaminonaphthalene-sulfonyl-polymyxin B (dansyl-PX), we were able to prove the intracellular accumulation of PX. A preliminary report has been presented (37).

An additional structural change, the formation of blebs in the outer membrane of gram-negative bacteria (9, 13, 31, 40), was reinvestigated by the application of spray-freezing and freeze-etching (1, 2, 24). Freeze-etching has been described for *Escherichia coli* B to give a relatively close approximation to the living state (5). It could be excluded that PX-induced

bleb formation is an artifact of fixation of detergent-weakened membranes. The technique used suggests these blebs to be evaginations of the cell surface monolayer of *Salmonella typhimurium*.

### MATERIALS AND METHODS

**Bacterial strains and culture conditions.** *S. typhimurium* SL 1135 (complete O-antigenic side chain of LPS) and SL 1102 (chemotype Re) were obtained from S. Schlecht, Max-Planck-Institut für Immunbiologie, Freiburg (Germany). *S. typhimurium* G 30 (a uridine 5'-diphosphate-galactose-4-epimerase-lacking mutant, chemotype Rc) was provided by M. J. Osborn, University of Connecticut at Farmington. *S. typhimurium* SL 1102-RE was a polymyxin-resistant mutant isolated in our laboratory (B. Bowman, Diploma thesis, Technical University of Munich, Munich, Germany, 1973). The filamentous *E. coli* B was isolated from the strain kept in the collection of our laboratory.

For all experiments, the cells were grown at 37 C with rapid shaking into logarithmic phase (optical density units, 0.66 at 600 nm; about  $7.5 \times 10^8$  cells/ml) in a glycerol-salts medium (32), which was supplemented with 0.3% casein-hydrolysate (Merck) and 0.01% each glycine, L-methionine, L-serine, and L-tryptophan.

**MICs.** Minimum inhibitory concentrations (MICs) were determined by inoculating bacterial cultures at 0.66 optical density units at 600 nm for 2 h with the antibiotic under growth-permitting conditions. The MIC was defined as the concentration of the antibi-

otic which just inhibited further growth of the bacteria.

**Microscopy.** For fluorescence microscopy, a Carl Zeiss Standard RA instrument was used. The desired concentration of dansyl-PX was added directly into the medium.

For freeze-etching, cells of *S. typhimurium* SL 1135 and G 30 were incubated with 10  $\mu\text{g}$  of PX per ml of medium for 3 min, centrifuged at 4 C for 10 min at  $3,000 \times g$ , washed once in distilled water, and resuspended to  $10^{10}$  cells/ml in distilled water. Further treatment of this suspension followed the method of Bachmann and Schmitt exactly (1).

**Preparation of dansyl-PX.** PX-sulfate (Pfizer) (40 mg) in 1.2 ml of 0.1 M  $\text{NaHCO}_3$  was incubated with 10 mg of dansylchloride (Serva) in 0.8 ml of acetone, without stirring, in the dark for 90 min at room temperature. The supernatant was applied onto a Sephadex G25 super-fine column (50 by 2.5 cm) and eluted with 0.145 M NaCl in 0.01 M sodium phosphate buffer, pH 7.1. A peak which showed orange fluorescence under ultraviolet light contained the dansyl-PX. This derivative could be extracted from the pooled fractions with *n*-butanol. After removal of the solvent in vacuo at 40 C, we obtained dansyl-PX as a pale yellow powder without contamination by other reaction products, as revealed by thin-layer chromatography (Merck, DC-Alurolle cellulose; solvent: *n*-butanol-pyridine-water-acetic acid, 60:40:30:3 [vol/vol/vol/vol].) The amount of dansyl-PX was determined by dinitrophenylation (3). The extinction coefficient  $\epsilon_{327.5}$  of dansyl-PX in distilled water was  $4.55 \times 10^4/\text{cm}^2$  per mol, which agrees well with protein-bound dansyl groups (42).

## RESULTS

**MICs of dansyl-PX as compared to PX.** The substitution of one amino group of PX by one dansyl group resulted in a significant decrease of bactericidal activity. As this activity is not diminished in mono-*N*-acetyl-PX derivatives (36), the decrease may be ascribed to the bulkiness of the comparably large dansyl group. Possibly, there is a preference of *N*-substitution in the cyclic part of the PX molecule. The latter is necessary for bactericidal activity (17). The MICs for some bacterial strains are summarized in Table 1.

**Fluorescence microscopy of Salmonella and Escherichia strains after treatment with dansyl-PX.** Cells grown in glycerol-salts medium were supplemented with the desired concentration of dansyl-PX. Immediately after application of the antibiotic, 50  $\mu\text{l}$  of the suspension was placed onto a slide, covered, and viewed under the microscope at room temperature.

If the experiment was performed at room temperature, all cells revealed fluorescence of their envelopes 30 s after dansyl-PX application, which was the fastest possible time of

TABLE 1. MICs in glycerol-salts medium of mono-*N*-dansyl-PX and PX and the ratio of these MICs in different strains of *S. typhimurium* and *E. coli* B

Strain	MIC		Ratio (PX/dansyl-PX)
	PX ( $\mu\text{g}/\text{ml}$ )	Dansyl-PX ( $\mu\text{g}/\text{ml}$ )	
<i>S. typhimurium</i>			
SL 1102	2.4	7.5	0.32
G 30	4.2	12	0.35
SL 1135	8	21	0.38
SL 1102-RE 30	20	50	0.40
<i>E. coli</i> B			
Rod shaped	8	21	0.38
Filamentous	5	13.5	0.37

sample handling. If concentrations at the MIC or higher were employed, fluorescent aggregations were detectable in the cell interior. Their number varied between one and twelve in a single cell. Normally, the largest patches were to be seen at the poles of the bacteria.

In Fig. 1 and 2, *S. typhimurium* G 30 is shown immediately before and after the formation of aggregates. This aggregation occurred spontaneously in the whole cell population at about the same time (Table 2).

Cells kept at 0 C showed no fluorescence even at a twofold MIC and after 2 h of incubation. However, if these cells were allowed to warm up under the microscope at room temperature, fluorescent aggregations occurred (see last three lines of Table 2). In cells originally kept at 0 C and then allowed to warm up on the microscope, the envelopes began to become fluorescent at the same time and independently of antibiotic concentration, which points to a discrete temperature at which binding starts. Likewise, aggregate formation exhibited the same phenomenon. This temperature transition of PX uptake and susceptibility has also been demonstrated with a mono-*N*-acetyl-PX derivative and has been discussed in relation to the temperature transition points of phospholipids (36).

The appearance of the fluorescent aggregates in the cytoplasm as a consequence of bactericidal concentration of PX clearly proves the penetration of the antibiotic into the cells. These aggregations seem to be bound to the membrane, which is shown by the conversion of filamentous dansyl-PX-treated *E. coli* B into spheroplasts (Fig. 3 and 4) by the method of Teuber (33). This could strengthen the interpretation of PX-deoxyribonucleic acid complexes because deoxyribonucleic acid is attached to the cytoplasmic membrane (27). Other patches

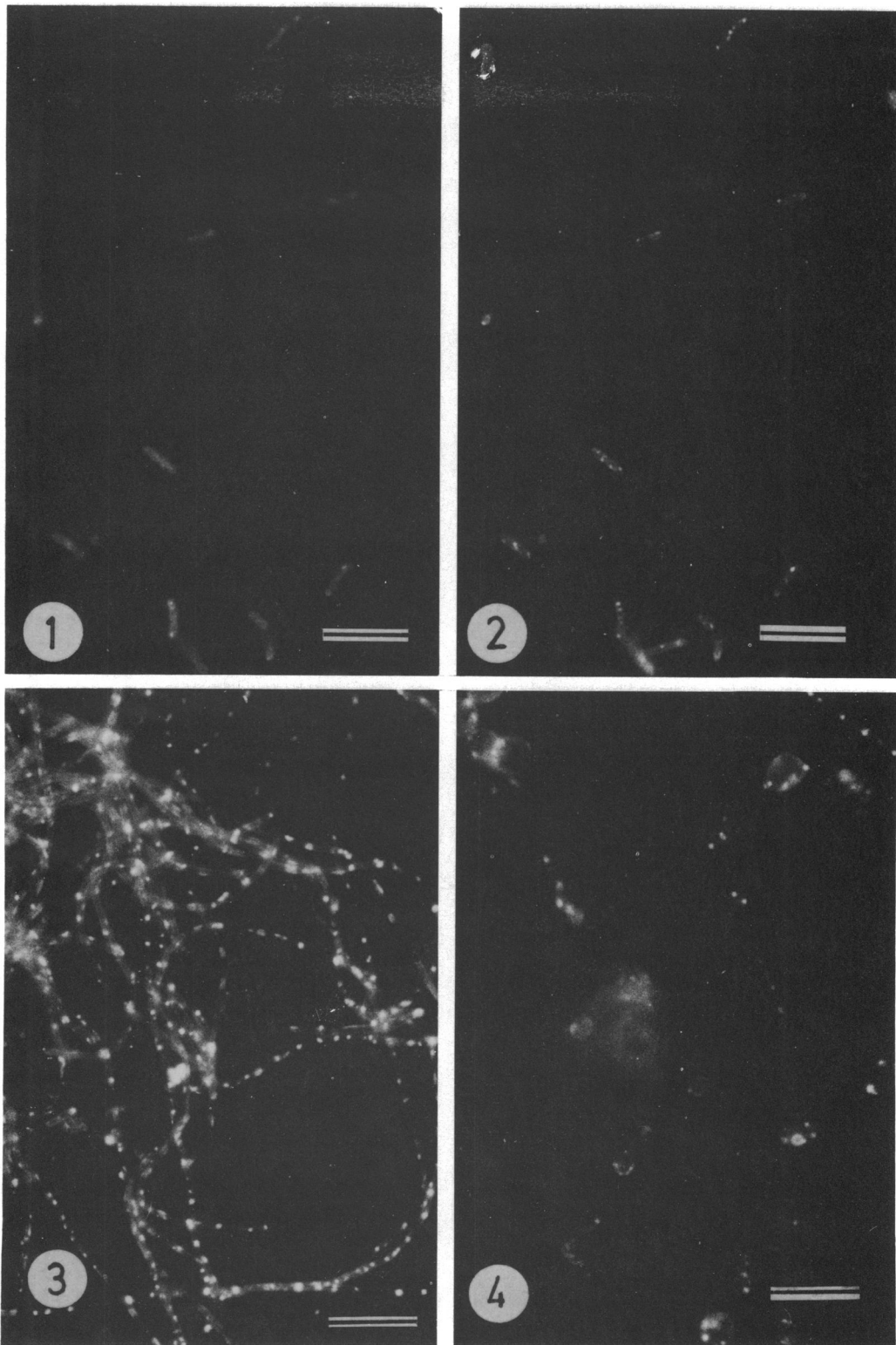


FIG. 1. Fluorescence of *S. typhimurium* G 30 after treatment with 18  $\mu\text{g}$  of dansyl-PX per ml at 0 C and subsequent transfer onto the microscope at 23 C. The formation of aggregations was just beginning. The bacteria were under the microscope 6 min. The bars in Fig. 1-6 represent 8  $\mu\text{m}$ .

FIG. 2. Same as in Fig. 1, but 1 min later.

FIG. 3. Aggregations with dansyl-PX in a filamentous *E. coli* B; treated with 21  $\mu\text{g}$  of dansyl-PX per ml for 3 min at 23 C.

FIG. 4. Same as in Fig. 3, but after addition of 50  $\mu\text{g}$  of lysozyme per ml for 10 min.

TABLE 2. *Fluorescence microscopy of S. typhimurium G 30<sup>a</sup>*

Temp (C)	Concn of dansyl-PX ( $\mu\text{g/ml}$ )	Appearance of fluorescence in cell envelopes	Appearance of fluorescent aggregations in the cell interior	Cells showing fluorescent aggregations (%)
23	2-6	At once	Not within 45 min	5
23	9	At once	Not within 45 min	10-15
23	12	At once	10-12 min	79-80
23	18	At once	1-2 min	100
23	24	At once	1 min	100
23	36	At once	0.5 min	100
37	6	At once	Not within 45 min	
37	12	At once	6-7 min	80
37	24	At once	0.5 min	100
0	6	3-4 min <sup>b</sup>	Not within 45 min	
0	12	3-4 min <sup>b</sup>	17-20 min <sup>b</sup>	70-80
0	24	3-4 min <sup>b</sup>	6-7 min <sup>b</sup>	100

<sup>a</sup> Time dependence of the envelope fluorescence and the formation of fluorescent aggregates in the cell interior after treatment with different concentrations of mono-*N*-dansyl-PX at different temperatures. The noted temperature is that of the bacterial suspension, the slides, and the antibiotic solution at the beginning of each experiment. The microscope temperature was always 23 C.

<sup>b</sup> Due to warming of the sample under the microscope.

may be complexes with ribonucleic acid and ribosomes as reported in vitro (19) or may represent a binding to mesosomes (25).

After a prolonged incubation of 1 h and longer, the amount and size of the fluorescent aggregations diminished. This is due to lysis of the bacteria (40), which includes severe degradation of nucleic acids (21, 35). The resulting disappearance of, mainly, the large aggregations is shown in Fig. 5.

Since the Zeiss Standard RA microscope enabled direct switching from fluorescence to phase-contrast microscopy settings, the internal, cytoplasmic localization of the fluorescent patches could be further established by focusing experiments using phase-contrast microscopy. Most of the fluorescent patches appear as dark aggregates in the interior of the cells (Fig. 6).

The described action of dansyl-PX on the bacterial cell (envelope fluorescence, formation, and loss of aggregates) was found in all tested strains (Table 1).

**Freeze-etching of *S. typhimurium* after treatment with PX.** Freeze-etching of untreated *S. typhimurium* G 30 revealed three

surface layers which were interpreted to consist of the relatively smooth upper monolayer of the outer membrane, the somewhat woven and finely particulated fracture face of the inner monolayer of the outer membrane, and the surface of the particulated rough cytoplasmic membrane (Fig. 7). The cytoplasm can be seen as a rough amorphous structure (Fig. 8). Our interpretation is based on the figures and their interpretation of *E. coli* (5, 20, 39) and of *Pseudomonas* and *Acinetobacter* (30, 38).

If the *S. typhimurium* G 30 cells were treated with 10  $\mu\text{g}$  of PX per ml for 3 min, numerous blebs appeared only at the outermost layer (smooth upper monolayer of the outer membrane) (Fig. 9-13). The PX-induced projections varied in size, with diameters between 10 and 30 nm. They appeared to be rather spherical in the 1-min etched samples (Fig. 9-11). In longer etched ones (3 min) they appeared to be "melted" to prolonged membranous eruptions (Fig. 12 and 13). They showed no regular pattern and varied between 200 and 500 globules/ $\mu\text{m}^2$ , as determined from Fig. 9. This distribution was also found in other samples. Assuming a mean number of 350 blebs/ $\mu\text{m}^2$  with a diameter of 20 nm, a surface enlargement of 11% would result by proposing half-spherical blebs. Spherical blebs would enlarge the surface area by 44% under the assumption that the cell dimensions, maintained by protein-protein and protein-phosphatidylethanolamine interactions, remain constant.

Freeze-etching of *S. typhimurium* SL 1135, having the complete polysaccharide chains of LPS, produced the same number of fracture faces. In addition, the outermost layer (smooth upper monolayer of the outer membrane) showed a rather complex structure (Fig. 14). A large number of "fibrils" originates from the smooth upper monolayer of the outer membrane. They extend to about 80 nm from the cell surface, which compares well with the length of the O-antigenic polysaccharide chains of LPS (4). Perhaps they represent LPS clusters. Their lack in *E. coli* B (20) is not surprising because this is a rough strain with surface structures like the rough *S. typhimurium* G 30 (chemotype Rc).

If *S. typhimurium* SL 1135 was treated with 10  $\mu\text{g}$  of PX per ml, blebs also formed in the outer leaflet of the outer membrane (Fig. 15 and 16). Some blebs seemed to arise from the base of one or more "fibrils" (Fig. 16).

## DISCUSSION

In this report, it is documented that the PX-induced aggregations of cytoplasmic material are dependent on bactericidal concentra-

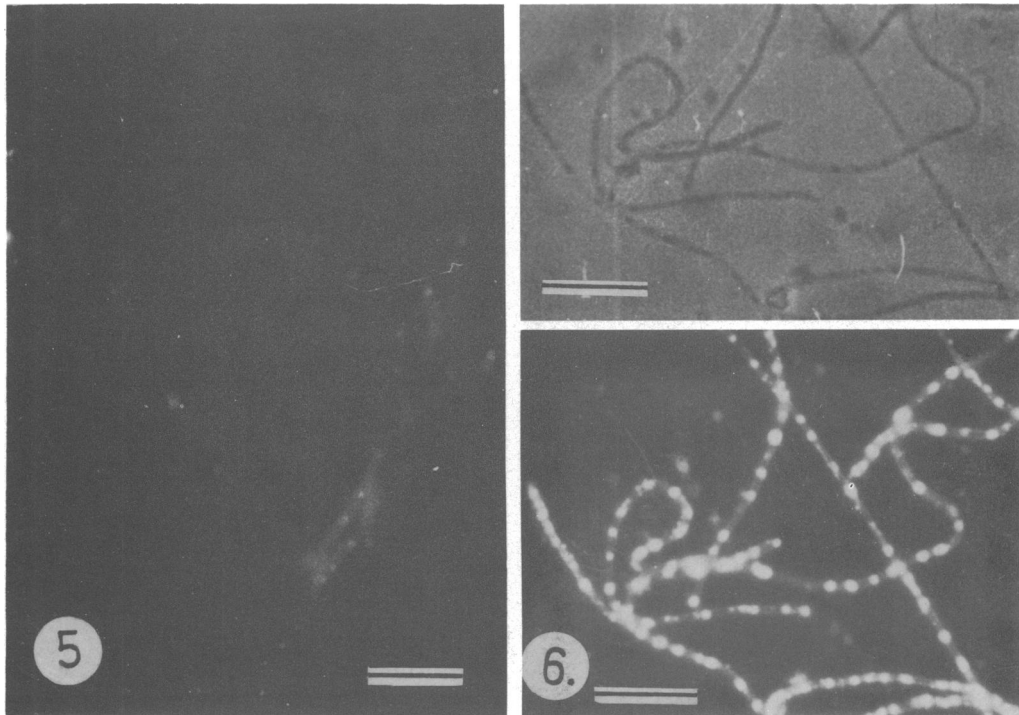


FIG. 5. Fluorescence of filamentous *E. coli B* after treatment with 21 µg of dansyl-PX per ml and incubation for 3 h at 23 C.

FIG. 6. Comparison of fluorescence and phase-contrast pictures of filamentous *E. coli B*. The sample was treated as described in Fig. 3. An identical area was photographed with a fluorescence setting (lower) and a phase-contrast setting (upper). Most fluorescent aggregations are also evident by phase-contrast microscopy as dark patches.

tions of the antibiotic. Though we have employed a derivative of the antibiotic, we believe that our findings are also valid for the natural PX molecule for two reasons. (i) The relative bactericidal activity of the dansyl derivative was the same for susceptible and more resistant strains. (ii) Aggregate formation in the cytoplasm was only induced by PX at bactericidal concentrations as revealed by phase-contrast microscopy (data not shown).

We suggest that these aggregations are due to a direct precipitation of nuclear material and ribosomes by the antibiotic (18, 19), but in what manner does PX penetrate into the cytoplasm and does this penetration occur at sublethal doses are questions that must be asked. It is possible that only at the MIC and higher is the accumulation of PX in the cytoplasm high enough to cause those aggregations. The response of PX-treated cells at sublethal concentrations might give valuable information. Sucrose-dependent plasmolysis, for example, was rapidly diminished at 25% of the MIC. At 50% of the MIC there was significant reduction of active transport, ribonucleic acid, deoxyribonucleic acid, and protein synthesis, and induction

of ribonucleic acid breakdown, as well as increased sensitivity to lysozyme (35). This is evidence for a destructive action of PX on the permeability barriers of the outer and cytoplasmic membranes. If we treated bacteria with sublethal doses of dansyl-PX, centrifuged, and added unlabeled PX to a lethal concentration, fluorescent aggregations were formed with decreased fluorescence intensity. This could be an indication that PX enters the cell at sublethal concentrations but is unable to precipitate cytoplasmic components. For ribosomes such a precipitation has been shown *in vitro* to be concentration dependent (19). Another interpretation is the possibility of transfer of envelope-bound PX into the cytoplasm if the antibiotic concentration is increased in the medium. Exchange of PX *in vitro* between isolated PX receptors is currently being investigated.

The formation of blebs was detected in the outermost layer of PX-treated cells. The cationic detergent chlorhexidine produces similar morphological alterations in gram-negative bacteria (15). Severe changes in the shape of erythrocytes after treatment with cationic and

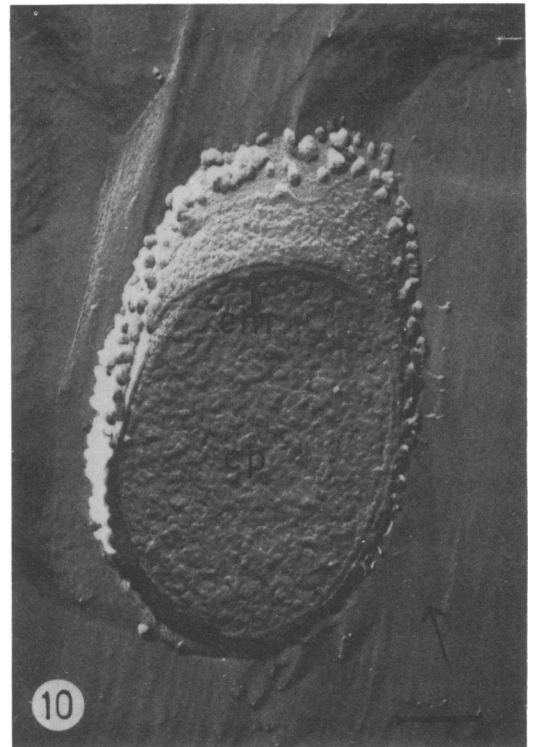
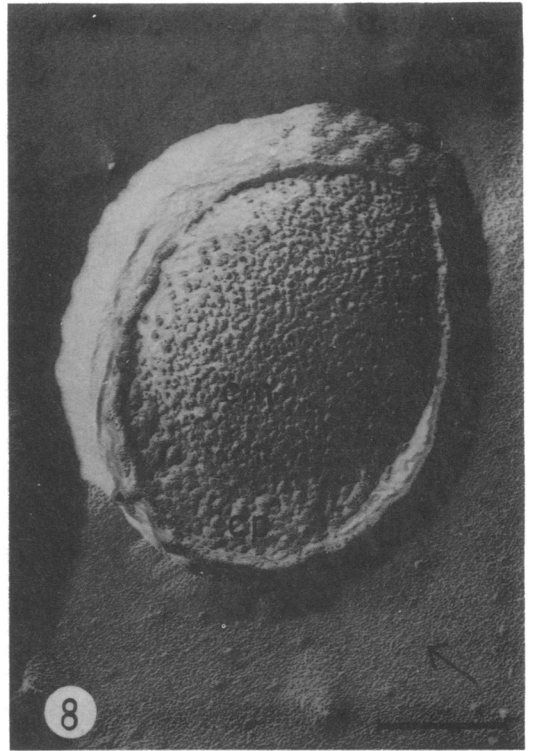
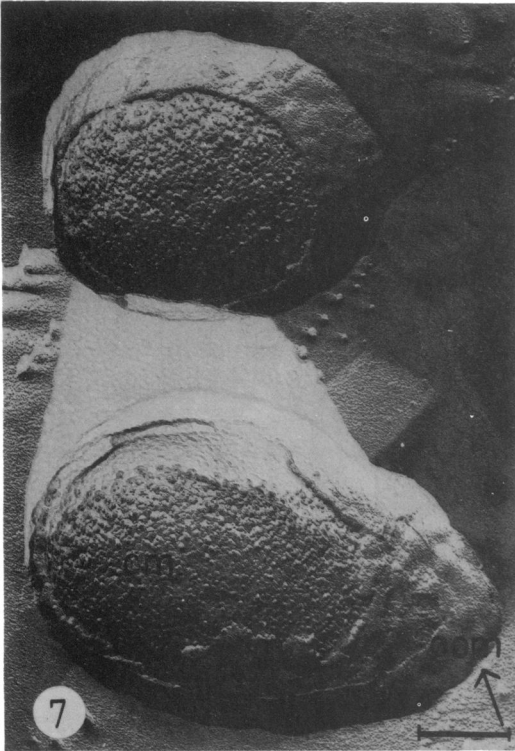


FIG. 7. Freeze-etching of *S. typhimurium* G 30 without PX treatment and after 1-min etching. Abbreviations: oom, outer monolayer of the outer membrane; iom, inner monolayer of the outer membrane; cm, outer surface of the plasma membrane. The arrow indicates the direction of shadowing. The marker bar represents 200 nm.

FIG. 8. Same as in Fig. 7; cp, cytoplasm.

FIG. 9. and 10. Freeze-etching of *S. typhimurium* G 30 after treatment with 10 µg of PX per ml for 3 min at 23 C; 1-min etching.



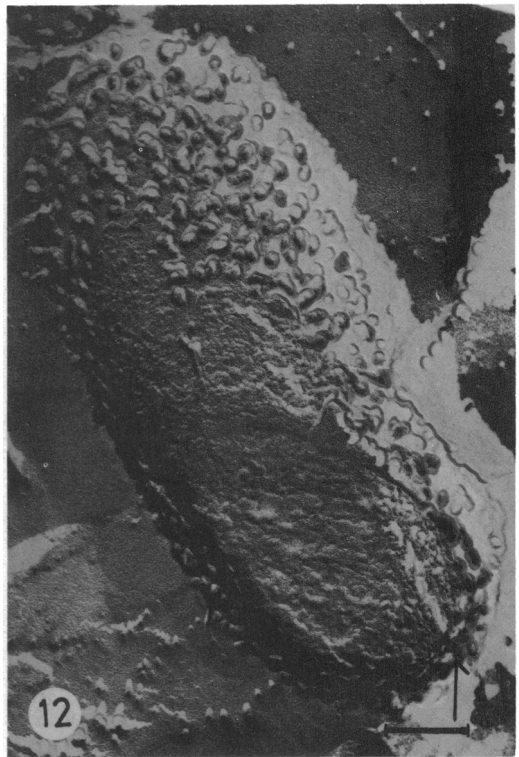
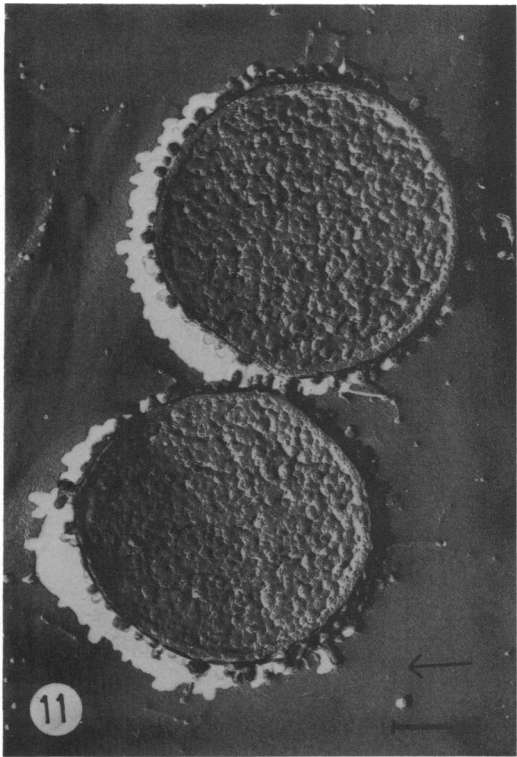


FIG. 11. Same as Fig. 9 and 10 showing cross-fractured cells.  
FIG. 12 and 13. Same as Fig. 9 and 10; 3-min etching.

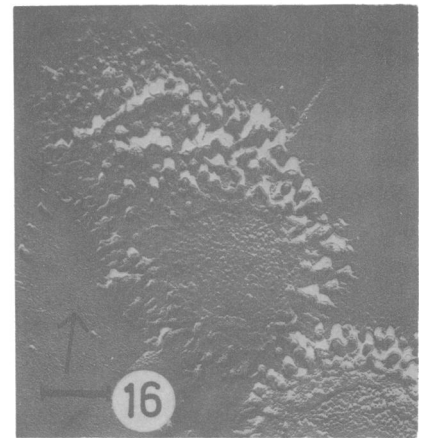
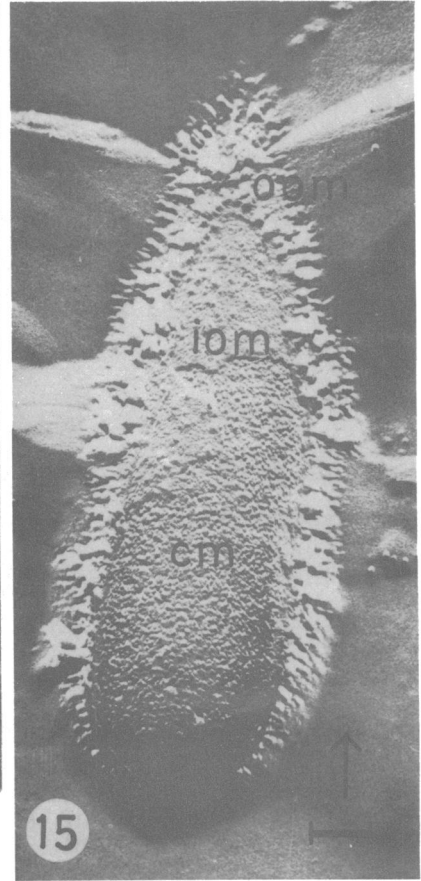
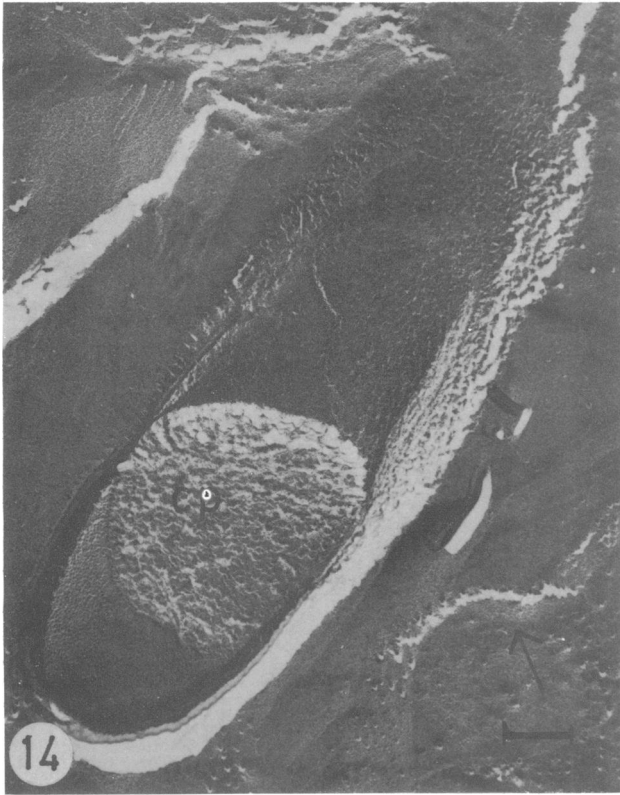


FIG. 14. Freeze-etching of *S. typhimurium* SL 1135 without PX treatment. Many "fibrils" arise from the outer leaflet; 1-min etching.

FIG. 15. Freeze-etching of *S. typhimurium* SL 1135 treated with 10 µg of PX per ml for 3 min at 23 C; 1-min etching.

FIG. 16. Same as in Fig. 15; blebs can arise from the basis of one or more "fibrils."

anionic drugs were interpreted as an intercalation of these drugs into either the outer or the inner monolayer of the membrane (28).

Few and Schulmann (7) demonstrated that

one molecule of polymyxin E occupies an area of 1.6 nm<sup>2</sup>. Suggesting a surface area of about 6 µm<sup>2</sup> for *S. typhimurium*, the intercalation of 2 × 10<sup>5</sup> molecules of PX per single cell (36) would



extend the surface by about 5% (35). The calculated enlargement of at least 11% can therefore not be explained by a simple intercalation of PX. In addition, extensive aggregations of membrane compounds must be postulated which will finally result in the bleb formation.

In *S. typhimurium* the lipid A part of LPS and the acidic phospholipids phosphatidylglycerol and cardiolipin are components of the outer membrane (16, 22) and known to complex with PX (3, 34). Of these substances, LPS is most likely asymmetrically localized only in the outer leaflet (8, 14), which is unknown for phosphatidylglycerol and cardiolipin. The described bleb formation could therefore be attributed to aggregations of PX with LPS, cardiolipin, and phosphatidylglycerol. This interpretation is supported for LPS by the observation that previous adsorption of LPS-specific phages prevented the PX-induced projections (12). Induction of bleb formation by PX has also been obtained with isolated cell envelopes (13). The aggregation of LPS and/or acidic phospholipids with PX at the site of bleb formation could lead to an extraction of these molecules from the remaining protein lattice. In this way we can envisage the production of pores, which must be large enough to account for the fact that PX-treated cells become permeable for proteins like lysozyme (33, 41) and periplasmic enzymes (6). Since molecules of the size of PX are usually not able to pass the outer membrane (23, 29), this mechanism would also explain the penetration of the antibiotic to the cytoplasmic membrane and into the cytoplasm.

Further elucidation of the PX action and penetration through the membranes of gram-negative bacteria must await investigations on the immediate environments of the antibiotic molecule in these membranes. The problem could be approached by the application of chemical cross-linking agents which produce a covalent linkage between PX and its neighbor molecules. Suitable agents are currently being investigated in our laboratory.

#### ACKNOWLEDGMENTS

We thank W. W. Schmitt-Fumian for the performance of freeze-etching and for helpful discussions.

This work was supported in part by the Deutsche Forschungsgemeinschaft, Bonn-Bad Godesberg.

#### LITERATURE CITED

- Bachmann, L., and W. W. Schmitt. 1971. Improved cryofixation applicable to freeze-etching. *Proc. Natl. Acad. Sci. U.S.A.* **68**:2141-2152.
- Bachmann, L., and W. W. Schmitt-Fumian. 1973. Spray-freezing and freeze-etching, p. 73-79. *In* E. L. Benedetti and P. Favard (ed.), *Freeze-etching, techniques and applications*. Soc. Francaise de Microscopie Electronique, Paris.
- Bader, J., and M. Teuber. 1973. Action of polymyxin B on bacterial membranes. I. Binding to the O-antigenic lipopolysaccharide of *Salmonella typhimurium*. *Z. Naturforsch. Teil C* **28**:422-430.
- Bayer, M. E. 1974. Ultrastructure and organization of the bacterial envelope. *Ann. N.Y. Acad. Sci.* **235**:6-28.
- Bayer, M. E., and C. C. Remsen. 1970. Structure of *Escherichia coli* after freeze-etching. *J. Bacteriol.* **101**:304-313.
- Cerny, G., and M. Teuber. 1971. Differential release of periplasmic versus cytoplasmic enzymes from *Escherichia coli* B by polymyxin B. *Arch. Mikrobiol.* **78**:166-179.
- Few, A. V., and J. H. Schulmann. 1953. The absorption of polymyxin E by bacteria and bacterial cell walls and its bactericidal action. *J. Gen. Microbiol.* **9**:454-466.
- Glauert, A. M., and M. J. Thornley. 1969. The topography of the bacterial cell wall. *Annu. Rev. Microbiol.* **23**:159-198.
- Handley, P. S., L. B. Quesnel, and M. M. Sturgiss. 1974. Ultrastructural changes produced in *Proteus vulgaris* by a synergistic combination of colistin and sulphadiazine. *Microbios* **10**:211-223.
- Hsu Chen, C. C., and D. S. Feingold. 1973. The mechanism of polymyxin B action and selectivity towards biologic membranes. *Biochemistry* **12**:2105-2111.
- Imai, M., K. Inoue, and S. Nojima. 1975. Effect of polymyxin B on liposomal membranes derived from *Escherichia coli* lipid. *Biochim. Biophys. Acta* **375**:130-137.
- Koike, M., and K. Iida. 1971. Effect of polymyxin on the bacteriophage receptors of the cell walls of gram-negative bacteria. *J. Bacteriol.* **108**:1402-1411.
- Koike, M., K. Iida, and T. Matsuo. 1969. Electron microscopic studies on the mode of action of polymyxin. *J. Bacteriol.* **97**:448-452.
- Leive, L. 1974. The barrier function of the Gram-negative envelope. *Ann. N.Y. Acad. Sci.* **235**:109-129.
- Longworth, A. R. 1971. Chlorhexidine, p. 95-106. *In* W. B. Hugo (ed.), *Inhibition and destruction of the microbial cell*. Academic Press Inc., New York.
- Mizushima, S., and H. Yamada. 1975. Isolation and characterization of two membrane preparations from *Escherichia coli*. *Biochim. Biophys. Acta* **375**:44-53.
- Nakajima, K. 1967. Structure-activity relationship of colistins. *Chem. Pharm. Bull.* **15**:1219-1224.
- Nakajima, K., and J. Kawamata. 1965. Studies on the mechanisms of action of colistin. I. Formation of an insoluble complex with nucleic acids. *Biken J.* **8**:225-231.
- Nakajima, K., and J. Kawamata. 1966. Studies on the mechanisms of action of colistin. III. Precipitation of *Escherichia coli* ribosomes with colistin. *Biken J.* **9**:45-50.
- Nanninga, N. 1970. Ultrastructure of the cell envelope of *Escherichia coli* B after freeze-etching. *J. Bacteriol.* **101**:297-303.
- Newton, B. A. 1956. The properties and mode of action of the polymyxins. *Bacteriol. Rev.* **20**:14-27.
- Osborn, M. J., J. E. Gander, E. Parisi, and J. Carson. 1972. Mechanism of assembly of the outer membrane of *Salmonella typhimurium*. I. Isolation and characterization of cytoplasmic and outer membranes. *J. Biol. Chem.* **247**:3962-3972.
- Payne, J. W., and C. Gilvarg. 1968. Size restriction on peptide utilization in *Escherichia coli*. *J. Biol. Chem.* **243**:6291-6294.
- Plattner, H., W. W. Schmitt-Fumian, and L. Bachmann. 1973. Spray-freezing of single cells, p. 81-100. *In* E. L. Benedetti and P. Favard (ed.), *Freeze-etching, techniques and applications*. Soc. Francaise de Microscopie Electronique, Paris.
- Pontefract, R. D., G. Bergeron, and F. S. Thatcher. 1969.

- Mesosomes in *Escherichia coli*. *J. Bacteriol.* **97**:367-375.
26. Rifkind, D. 1967. Studies on the interaction between endotoxin and polymyxins. *J. Infect. Dis.* **117**:433-438.
  27. Ryter, A. 1968. Association of the nucleus and the membrane of bacteria: a morphological study. *Bacteriol. Rev.* **32**:39-54.
  28. Sheetz, M. P., and S. J. Singer. 1974. Biological membranes as bilayer couples. A molecular mechanism of drug-erythrocyte interactions. *Proc. Natl. Acad. Sci. U.S.A.* **71**:4457-4461.
  29. Singh, A. P., K.-J. Cheng, J. W. Costerton, E. S. Idziak, and J. M. Ingram. 1972. Sensitivity of normal and mutant strains of *Escherichia coli* to actinomycin-D. *Can. J. Microbiol.* **18**:909-915.
  30. Sleytr, U. B., M. J. Thornley, and A. M. Glauert. 1974. Location of the fracture faces within the cell envelope of *Acinetobacter* species strain MJT/F5/5. *J. Bacteriol.* **118**:693-707.
  31. Suganuma, S., K. Hara, T. Kishida, K. Nakajima, and J. Kawamata. 1968. Cytological changes of *Escherichia coli* caused by polymyxin E. *Biken J.* **11**:149-155.
  32. Teuber, M. 1969. Phosphorylation of methyl- $\alpha$ -D-glucopyranoside in polymyxin B-treated *Salmonella typhimurium*. *J. Bacteriol.* **100**:1417-1419.
  33. Teuber, M. 1970. Lysozyme-dependent production of spheroplast-like bodies from polymyxin B-treated *Salmonella typhimurium*. *Arch. Mikrobiol.* **70**:139-146.
  34. Teuber, M. 1973. Action of polymyxin B on bacterial membranes. II. Formation of lipophilic complexes with phosphatidic acid and phosphatidyl-glycerol. *Z. Naturforsch. Teil C* **28**:476-477.
  35. Teuber, M. 1974. Action of polymyxin B on bacterial membranes. III. Differential inhibition of cellular functions in *Salmonella typhimurium*. *Arch. Microbiol.* **100**:131-144.
  36. Teuber, M., and J. Bader. 1971. Quantitative correlation of uptake with antibiotic activity of polymyxin B in *Salmonella typhimurium*. *FEBS Lett.* **16**:195-197.
  37. Teuber, M., J. Bader, P. Schindler, and B. F. Bowman. 1974. Wirkung des Polymyxin B auf die Membranen und Membrankomponenten von *Salmonella typhimurium*. *Zentralbl. Bakteriol. Parasitenkd. Infektionskr. Hyg. Abt. 1 Orig. Reihe A* **228**:243-245.
  38. Thornley, M. J., and U. B. Sleytr. 1974. Freeze etching of the outer membranes of *Pseudomonas* and *Acinetobacter*. *Arch. Microbiol.* **100**:409-417.
  39. Van Gool, A. P., and N. Nanninga. 1971. Fracture faces in the cell envelope of *Escherichia coli*. *J. Bacteriol.* **108**:474-481.
  40. Wahn, K., G. Lutsch, T. Rockstroh, and K. Zapf. 1968. Morphological and physiological investigations of the action of polymyxin B on *Escherichia coli*. *Arch. Mikrobiol.* **63**:103-116.
  41. Warren, G. H., J. Cray, and J. A. Yurchenco. 1957. Effect of polymyxin on the lysis of *Neisseria catarrhalis* by lysozyme. *J. Bacteriol.* **74**:788-793.
  42. Weber, G. 1952. Polarization of the fluorescence of macromolecules. 2. Fluorescent conjugates of ovalbumin and bovine serum albumin. *Biochem. J.* **51**:155-167.